Inorganic Chemistry

Article

pubs.acs.org/IC

Toward New Organometallic Architectures: Synthesis of Carbene-Centered Rhodium and Palladium Bisphosphine Complexes. Stability and Reactivity of $[PC^{BIm}PRh(L)][PF_6]$ Pincers

Andriy Plikhta, Alexander Pöthig, Eberhardt Herdtweck, and Bernhard Rieger*

WACKER-Lehrstuhl für Makromolekulare Chemie & Catalysis Research Center, Technische Universität München, Lichtenbergstraße 4, 85748 Garching b. München, Germany

Supporting Information

ABSTRACT: In this article, we report the synthesis of a tridentate carbene-centered bisphosphine ligand precursor and its complexes. The developed four-step synthetic strategy of a new $PC^{BIm}P$ pincer ligand represents the derivatization of benzimidazole in the first and third positions by (diphenylphosphoryl)methylene synthone, followed by phosphine deprotection and subsequent insertion of a non-coordinating anion. The obtained ligand precursor undergoes complexation, with $PdCl_2$ and $[\mu\text{-}OCH_3Rh(COD)]_2$ smoothly forming the target organometallics $[PC^{BIm}PPdCl][PF_6]$ and $[PC^{BIm}PRh(L)][PF_6]$ under mild hydrogenation conditions. A more detailed study of the rhodium complexes $[PC^{BIm}PRh(L)][PF_6]$ reveals significant thermal stability of the $PC^{BIm}PRh$ moiety in the solid state as well as in solution. The chemical behavior of 1,3-bis(diphenylphosphinomethylene)benzimidazol-2-ylrhodium acetonitrile hexafluorophosphate has been screened under decarbonylation, hydrogenation, and hydroboration reaction conditions. Thus, the $PC^{BIm}PRh^{I}$ complex is a sufficiently stable compound, with the potential to be applied in catalysis.

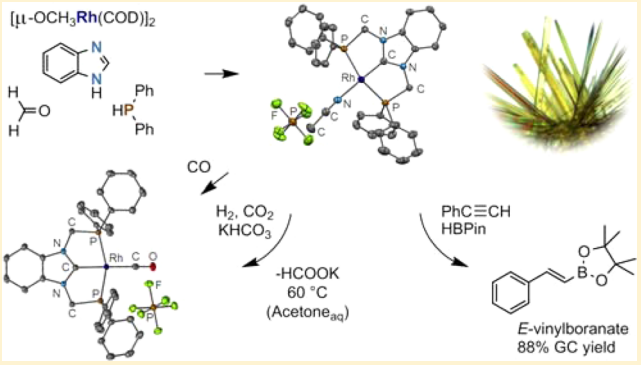

INTRODUCTION

Research on N-heterocyclic carbenes (NHCs) is an exponentially growing area nowadays. Owing to their easy accessibility, strong coordinating character, oxidation resistance, and high thermal stability of their metal complexes, the NHCs serve as a powerful tool in different research fields[1−5] and are promising ligands for industrially relevant areas.[4,6−9] Metal−carbene bonds in transition-metal NHC organometallics determine their remarkable catalytic performance in olefin metathesis,[2,10] hydrogenation reactions,[11,12] hydroformylation[13] and others.[5,14] In spite of the broad structural diversity of known NHCs, a search for new architectures and their application fields continues steadily.[7,11,15−18] Carbene-based pincer complexes[19,20] have shown their high potential for various catalytic reactions such as C−C and C−X couplings[4,21,22] or alkene isomerization,[23] but examples of their application as catalysts are still rather rare. Notably, the nature of tridentate equatorial ligands allows strong retention of the metal core, resulting in a high thermodynamic stability of the pincers[24] and opens a range of novel catalytic approaches. The most pronounced among them are acceptorless dehydrogenation of alkanes,[25−27] transfer (de)hydrogenation,[28,29] alkane metathesis,[30] carbon dioxide (CO_2) hydrogenation,[31−34] and further applications.[21,35−39] Moreover, in some cases, the ligand constitution has a crucial impact on the behavior of the catalytic active species, enabling new reaction pathways through ligand−metal cooperation.[40−43] At the same time, the role of five-membered heterocyclic ligands, their electronic properties, their reactivity, and in particular their cooperative interactions in catalytic processes are of significant interest and have not been studied yet to the full extent. Therefore, we focused our attention on the synthetic accessibility and reactivity of the carbene-centered pincer complexes.

While the [5,5]-membered boron,[44−46] [6,6]/[5,5]-membered nitrogen,[47−49] [5,5]-membered silicon,[50,51] [5,5]-triazole,[52] triazolylidene,[53] and [6,6]-(benz)imidazolium[54−57] carbon-centered phosphine-functionalized pincer complexes were discovered during the past decade, the carbene-based [5,5]-(benz)imidazolium type has remained a challenge (Figure 1).[58]

In this work, we report for the first time the synthesis of a cationic phosphine-functionalized methylene-bridged tridentate benzimidazolin-2-ylidene ligand precursor, its $PC^{BIm}PPd^{II}$ and $PC^{BIm}PRh^{I}$ complexes, as well as the stability study of $PC^{BIm}PRh^{I}$ and evaluation of its chemical behavior in various environments. By combining the features of both the strong σ-donating properties of the NHC moiety and the tridentate equatorial complexation mode of the ligands, we present a new tool for organometallic chemistry.

Received: June 29, 2015
Published: September 21, 2015

DOI: 10.1021/acs.inorgchem.5b01428
Inorg. Chem. 2015, 54, 9517−9528

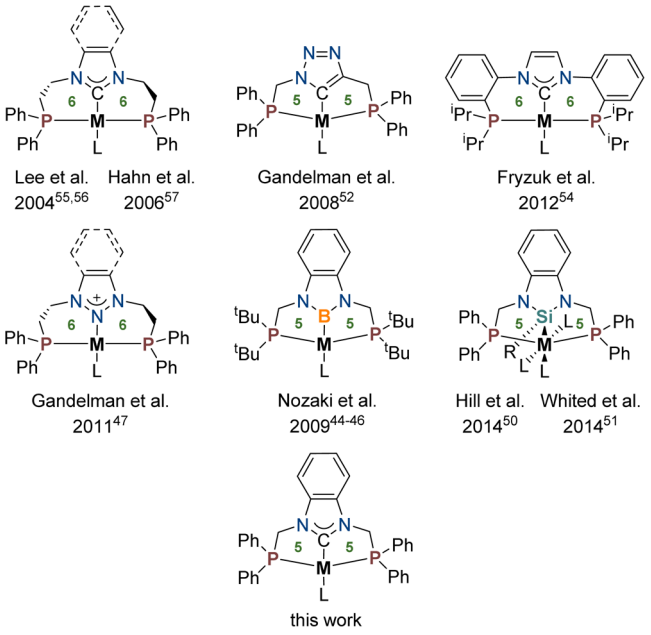

Figure 1. Recent developments in heterocyclic-based bisphosphine metal complexes.[59]

RESULTS AND DISCUSSION

The accessibility of [5,5]-membered $PC^{BIm}P$ metal complexes has been a challenge because of the complexity of the synthesis of a 1,3-bis(diphenylphosphinomethylene)benzimidazolium architecture rather than metal insertion. According to the retrosynthetic analysis represented in Scheme 1, the target ionic ligand precursor can be obtained in four steps, starting from commercially available benzimidazole, diphenylphosphine, and formaldehyde. Upon analysis of the critical points of the retrosynthesis, it should be noted that we were not able to perform N-alkylation of benzimidazole in the third position using CH_2Cl_2, CH_2ICl, and CH_2Br_2. This would allow consecutive halogen substitution in the halogenomethylene-benzimidazole moiety by the diphenylphosphine group with formation of the target molecule. The strong electron-acceptor properties of phosphine oxides as well as the steric influence of the tosylate leaving group, which determines the reactivity of the *p*-toluenesulfonyl derivative,[60] were considered to build a methylene bridge between phosphorus and nitrogen heteroatoms.[58,61,62] Therefore, methylenediphenylphosphinoxide synthone was chosen for N-quarternization. Another problematic issue was deprotection of phosphine oxide, leading to the target molecule. Such reduction takes place normally under relatively harsh conditions but theoretically was evident, proceeding from numerous reports: $AlH(^iBu)_2$,[63] AlH_3,[64] $MeX/LiAlH_4$,[65] $PhSiH_3$,[66,67] $SiHCl_3$,[68−70] $Ti(O^iPr)_4$/poly(methylhydrosiloxane) (PMHS),[71] $Ti(O^iPr)_4/HSi(OEt)_3$,[72] and [Cu]/(PMHS or tetramethyldisiloxane (TMDS)).[73] Herein, interaction of another reactive molecule site during the synthesis was expected as well.

Scheme 1. Retrosynthetic Analysis of Target Phosphine-Functionalized Methylene-Bridged Benzimidazolinium Salts

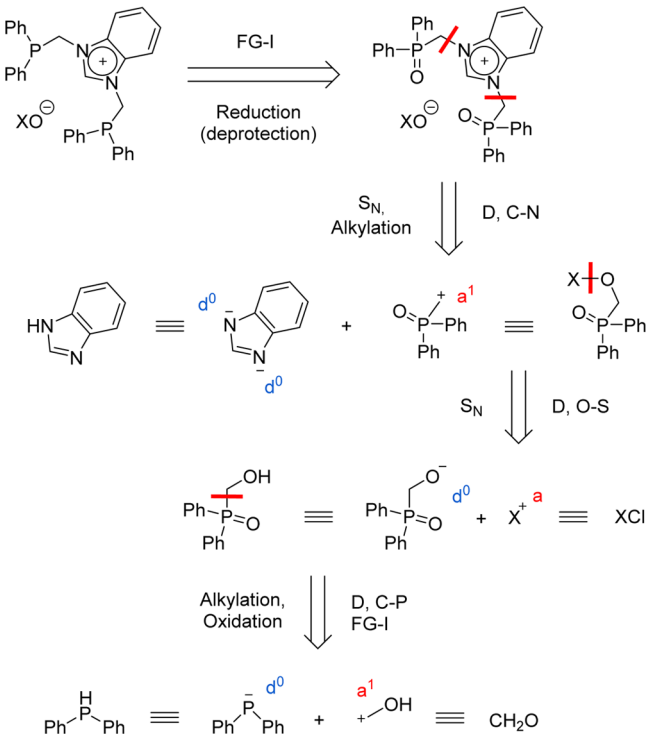

Metal insertion was aimed to be performed through the direct metalation of phosphine-functionalized benzimidazolium salt using the appropriate rhodium(I) methoxide or metal chloride precursor. Diphenyl substituents were chosen considering their less steric bulkiness compared to ^{i}Pr and ^{t}Bu. In this work, we set our choice on the normal carbene motif, blocking the fourth and fifth positions by an aromatic ring to prevent the abnormal coordination mode.[74−76] Although, it was expected that the abnormal carbenes might form more reactive catalytic species.[77−79]

[(Diphenylphosphoryl)methyl]-4-methylbenzenesulfonate (**1**) can be obtained with moderate yields according to the previous works.[60] We have significantly optimized and modified the synthesis of **1** to the gram scale with an overall yield of 71% [see the Supporting Information (SI)]. While the first alkylation of benzimidazole gives an almost quantitative yield of 1-[(diphenylphosphoryl)methylene]benzimidazole (**2**) in the presence of K_2CO_3 in dimethyl sulfoxide (DMSO), the second alkylation step could be performed only under neat conditions, slightly over the melting point of **1**. The obtained diphenylphosphoryl derivative 1,3-bis[(diphenylphosphoryl)-methylene]benzimidazolium 4-methylbenzylsulfonate (**3**) was then reduced using a $Ti(O^iPr)_4$/PMHS system.[71,80] This reaction is conducted by simultaneous hydrogenation of the benzimidazolium fragment, giving 1,3-bis(diphenylphosphinomethylene)benzimidazoline (**4**). The phosphine deprotection is highly dependent on reaction conditions. Thus, conducting the reaction over more than 3 h or increasing the temperature over 70 °C led to the formation of several byproducts in most of the cases because of decomposition of the reaction product. Interestingly, the use of $HSiCl_3$ as a reducing agent[75] led to hydrogenation of the only cationic moiety without P−O bond reduction under mild conditions. By testing several known synthetic dehydrogenation approaches[17,81−86] we have found that the most successful was the use of nonmetal-containing reagents, viz., triphenylcarbenium derivatives.[87,88] Thus, the target 1,3-bis(diphenylphosphinomethylene)benzimidazolium salt was obtained in one step by hydride abstraction from **4** with the simultaneous introduction of a noncoordinating hexafluorophosphate counterion (Scheme 2). Because of the ring-opening

DOI: 10.1021/acs.inorgchem.5b01428
Inorg. Chem. 2015, 54, 9517−9528

Scheme 2. Synthesis of 5

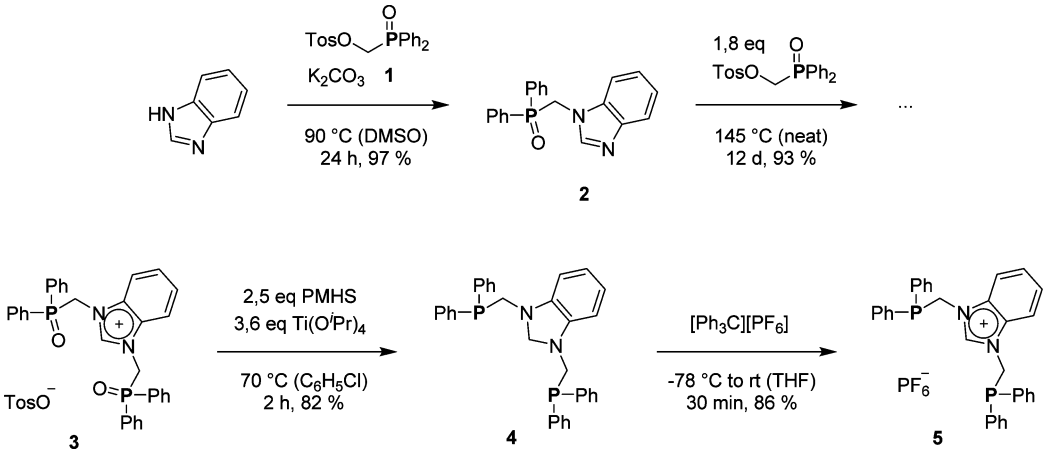

polymerization of tetrahydrofuran (THF) caused by $[(C_6H_5)_3C][PF_6]$, low temperatures (−78 °C) and short reaction times (30 min) are required.

The structure of the ligand precursor 1,3-bis-(diphenylphosphinomethylene)benzimidazolium hexafluorophosphate (**5**) was confirmed by NMR spectroscopy, mass spectrometry (MS), and elemental analysis (EA). Single-crystal X-ray analysis established the structural details of the methylene-bridged ligand precursor **5**, confirming formation of the desired proligand. The results are consistent with those reported for the PBP X-ray structure (Figure 2).[44]

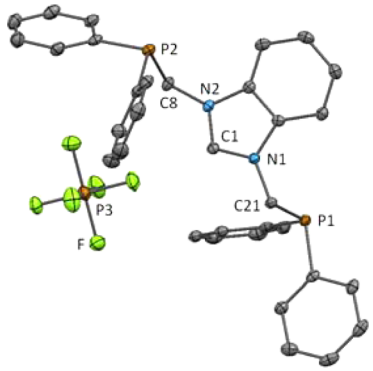

Figure 2. Crystal structure of **5** (50% displacement ellipsoids; hydrogen atoms were omitted for clarity). Selected interatomic distances (Å) and angles (deg): N1−C1, 1.3323(19); N2−C1, 1.3296(19); N1−C21, 1.4646(18); N2−C8, 1.4674(18); P1−C21, 1.8736(15); P2−C8, 1.8686(15); C1−N2−C8, 125.46(12); C1−N1−C21, 126.71(12); N1−C21−P1, 113.21(10); N2−C8−P2, 112.25(10).

The obtained organic salt **5** undergoes complexation with $[\mu\text{-}OCH_3Rh(COD)]_2$ smoothly through deprotonation of the benzimidazolium moiety, forming the target organometallic product $[PC^{BIm}PRh(solvent)][PF_6]$ (**6**) under mild hydrogenation conditions (Scheme 3). The use of simple inorganic metal halides like $PdCl_2$ as precursors for the synthesis of $PC^{BIm}P$-based organometallics was also tested. The palladium complex 1,3-bis(diphenylphosphinomethylene)benzimidazol-2-ylpalladium chloride hexafluorophosphate (**7**) was obtained by direct complexation without the addition of a base according to analogous procedures.[52,55]

Scheme 3. Synthesis of 6 and 7

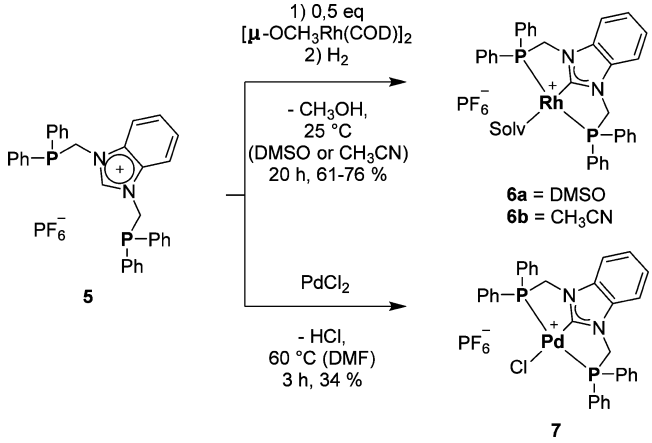

The structures of $PC^{BIm}PRh^{I}$ complexes **6a** and **6b** as well as $PC^{BIm}PPd^{II}$ complex **7** were confirmed by NMR, MS, IR, and X-ray techniques (see the SI). The following NMR chemical shifts give exhaustive evidence for complexation of these transition metals. Thus, the signal corresponding to the two phosphorus atoms shifts from −14.05 ppm (ligand precursor) to 45.84 ppm (d, J^{P-Rh} = 152.8 Hz) for the rhodium complex **6b** and to 38.16 ppm (singlet) for the palladium complex **7** in the ^{31}P NMR spectrum. The methylene protons were detected at 4.97 ppm (vt, J^{H-P} = 3.0 Hz) for **6b** and at 5.45 ppm (vt, J^{H-P} = 3.3 Hz) for **7** in the ^{1}H NMR spectrum, while the characteristic singlet of the acidic proton H2 at 8.69 ppm disappears in both cases during the reaction.

Single crystals suitable for X-ray crystallographic analysis were grown from DMSO/ethanol (Et_2O) and acetonitrile (CH_3CN)/Et_2O solutions. The structures of **6a**, **6b**, and **7** are presented in Figures 3 and 4. Hereby, because of the limited quality of the measured crystal, we do not discuss the molecular structure of **6a** in detail (for metrical data, see SI). A small fraction of the whole molecule disorder could not be resolved and yields residual electron densities of the second set of heavy atoms, which result in a checkcif A-alert. The $PC^{BIm}P$ pincer ligand coordinates meridionally upon reaction with the tested late-transition-metal precursors. The rhodium and palladium adopt a distorted square-planar geometry, which is consistent with the reported $PBPRh^{I}$ [45] and $PCPPd^{II}$ [52] X-ray structures. The fourth coordination site is occupied by a loosely bonded

DOI: 10.1021/acs.inorgchem.5b01428
Inorg. Chem. 2015, 54, 9517−9528

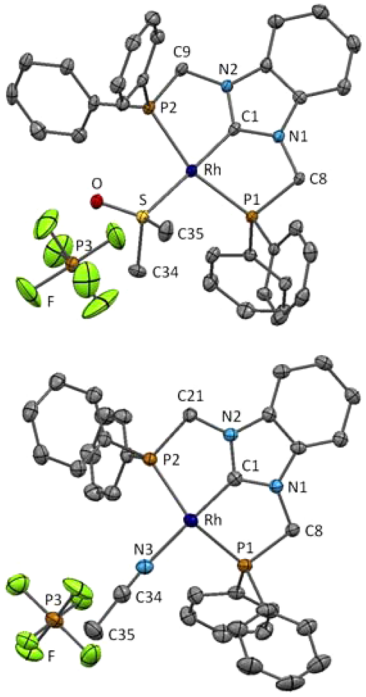

Figure 3. Crystal structures of **6a** (at the top) and **6b** (at the bottom) (50% displacement ellipsoids; hydrogen atoms were omitted for clarity). Selected interatomic distances (Å), angles (deg), and torsion angles (deg) for **6b**: Rh−N3, 2.091(3); Rh−C1, 1.933(3); Rh−P1, 2.2739(8); Rh−P2, 2.2976(8); N1−C1, 1.369(4); N2−C1, 1.365(4); N1−C8, 1.457(4); N2−C21, 1.457(4); P1−C8, 1.873(3); P2−C21, 1.860(3); N3−Rh−C1, 178.15(12); P1−Rh−P2, 155.28(3); N1−C1−N2, 106.0(3); Rh−P1−C8−N1, −6.18; Rh−P2−C21−N2, 21.64.

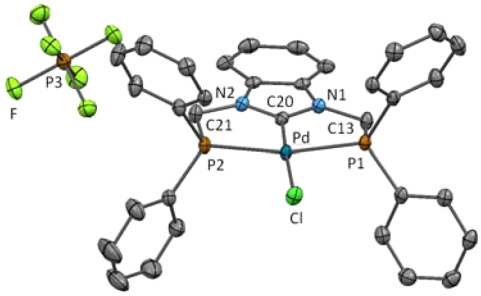

Figure 4. Crystal structure of **7** (50% displacement ellipsoids; hydrogen atoms were omitted for clarity). Selected interatomic distances (Å), angles (deg), and torsion angles (deg): Pd−Cl, 2.3381(5); Pd−C20, 1.9356(17); Pd−P1, 2.2924(5); Pd−P2, 2.3098(5); N1−C20, 1.346(2); N2−C20, 1.345(2); N1−C13, 1.457(2); N2−C21, 1.457(2); P1−C13, 1.8606(18); P2−C21, 1.8688(19); Cl−Pd−C20, 176.95(5); P1−Pd−P2, 162.76(2); N1−C20−N2, 108.06(14); Pd−P1−C13−N1, 16.16; Pd−P2−C21−N2, −2.33.

solvent molecule in **6a** and **6b** or by a halogen atom in **7** trans to the carbene. The heterocyclic rings in methylene-bridged **6b** and **7** are not twisted from the rhodium and palladium planes as was the case for the ethylene-bridged imidazole-centered[55,56] or phenylene-bridged dihydroimidazole-based bisphosphine complexes[54] and coordinate in a planar fashion to the metal center. The geometry of complex **7** is consistent with the calculated 1,3-bis(diphenylphosphinomethylene)imidazol-2-yl-palladium chloride reported by Lee et al.[55]

In this work, we have mainly focused on rhodium complexes, although the PC^{BIm}P palladium organometallic compounds undoubtedly deserve no less attention. Upon a study of the stability of **6a** and **7**, it was observed that the rhodium complexes were stable in the presence of moisture but underwent degradation in oxygen-containing environments, while the palladium complex **7** remained stable under moisture and air over weeks in solution.

Thermogravimetric analysis (TGA) of substances **5** and **6a** in the solid state shows that complexation of the metal by organic salt **5** leads to some stabilization of the carbon-heteroatom-alternated molecule architecture. While the PC^{BIm}P ligand precursor decomposes at an offset temperature of 221 °C with 97% mass loss, the rhodium complex undergoes degradation in three steps at 131, 258, and 513 °C with an overall mass loss of around 73% (Figure 5). The first degradation step up to 258 °C corresponds to the mass loss of coordinated DMSO (m/z 78; mass loss 9.29%), and subsequently other degradation products are released.

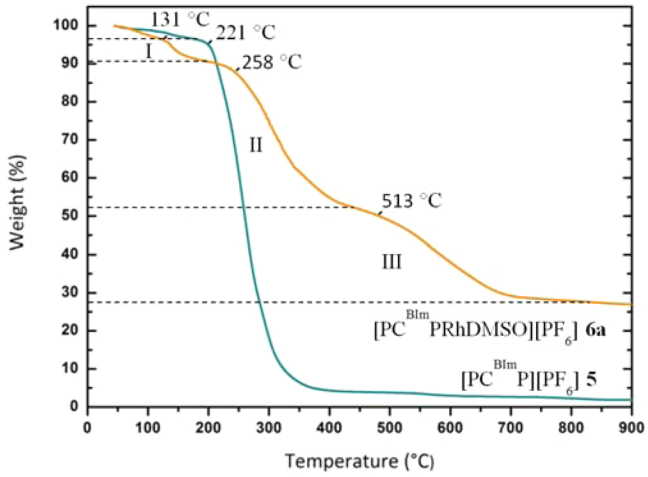

Figure 5. TGA of the PC^{BIm}P ligand precursor **5** and the PC^{BIm}PRh^{I} complex **6a**.

Furthermore, we were interested in exploring the chemistry of organometallic compound **6b** and determining its stability and reactivity in various environments, taking into account possible side reactions.

First, the interaction of **6b** with π-acceptor ligands was investigated (Scheme 4). The 16-electron square-planar rhodium carbonyl complex **8** was obtained by exposure of **6b** to a carbon monoxide (CO) atmosphere (1−10 bar) in propylene oxide (PO). On the other hand, ethylene binds reversibly to the rhodium atom in PO, dichloromethane (CH_2Cl_2), and THF at 25 °C, as observed by an in situ ^{31}P NMR experiment. After ethylene was added to the solutions of **6b**, a new doublet signal was detected at 61.29 ppm (d, J^{P-Rh} = 137.6 Hz), evidencing the formation of 1,3-bis(diphenylphosphinomethylene)benzimidazol-2-ylrhodium ethylene hexafluorophosphate (**9**; see the SI). However, the ethylene-coordinated complex could not be isolated from those polar solvents.

The coordination of CO causes the chemical shift of the phosphorus atoms from 45.84 ppm (d, J^{P-Rh} = 152.8 Hz) for **6b** to 55.41 ppm (d, J^{P-Rh} = 138.5 Hz) in the downfield of the ^{31}P NMR spectrum. In the ^{1}H NMR spectrum, the signal

DOI: 10.1021/acs.inorgchem.5b01428
Inorg. Chem. 2015, 54, 9517−9528

Scheme 4. Reactions of CO and ethylene with 6b[a]

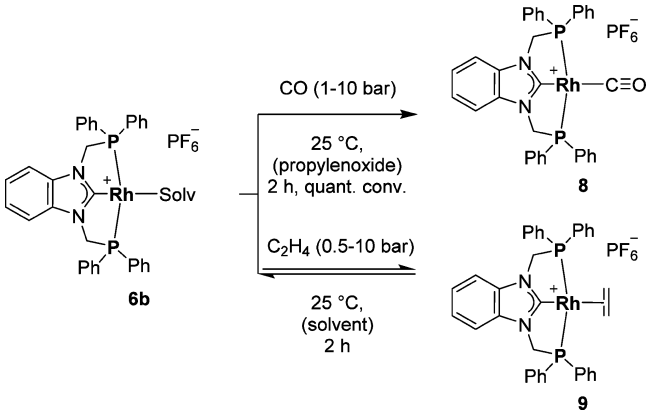

[a]Conversion is estimated by ^{1}H and ^{31}P NMR spectroscopy.

related to the methylene protons is also shifted downfield and appears at 5.37 ppm (vt, J^{H-P} = 3.1 Hz).

It is worth noting that the shift of all proton signals to the high-frequency field took place after CO was bonded to the metal center, evidencing an overall decrease of the electron density around the hydrogen atoms. In addition, the ^{13}C NMR chemical shift of the C2 nucleus changed from 198.96 ppm (dt, J^{C-Rh} = 51.2 Hz, $J^{2,C-P}$ = 11.9 Hz) to 197.21 ppm (dt, J^{C-Rh} = 40.5 Hz, $J^{2,C-P}$ = 12.6 Hz) to the upfield region for complex **8**. The singlet of the carbon-13 atom of the carbonyl group was detected at 195.96 ppm.

The light-yellow crystals of **8** suitable for X-ray analysis were grown by the addition of diethyl ether to the reaction mixture. The solid-state structure of **8** (Figure 6) represents the

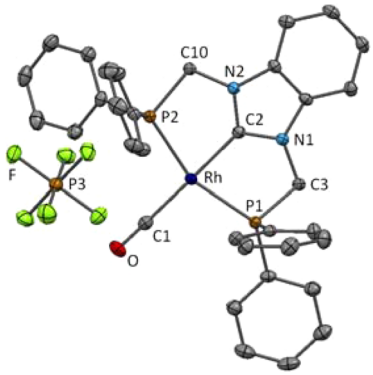

Figure 6. Crystal structure of **8** (50% displacement ellipsoids; hydrogen atoms were omitted for clarity). Selected interatomic distances (Å), angles (deg), and torsion angles (deg): Rh−C1, 1.8882(17); Rh−C2, 1.9994(15); Rh−P1, 2.3003(4); Rh−P2, 2.3093(4); N1−C2, 1.3521(19); N2−C2, 1.354(2); N1−C3, 1.4571(19); N2−C10, 1.4605(19); P1−C3, 1.8726(16); P2−C10, 1.8606(16); C1−O, 1.142(2); C1−Rh−C2, 178.80(7); P1−Rh−P2, 153.52(1); N1−C2−N2, 106.90(13); Rh−P1−C3−N1, 24.38; Rh−P2−C10−N2, −5.34.

expected distorted square-planar environment around rhodium. Powder IR spectroscopy showed the characteristic CO stretching band at 1995 cm^{-1}. This value indicates a medium electron-donating character of the $PC^{BIm}P$ ligand, which is comparable with that of the phosphaferrocene-pyrrole-based pincer ligand (ν = 1990 cm^{-1}) reported by Mathey et al.[48] The CO bond vibration of **8** is considerably higher than the values obtained for weak π-acceptor ligands $PC^{m\text{-phenylene}}P$[89] (ν = 1929 and 1943 cm^{-1}), $PC^{Im}P$,[56] and PBP[45] (ν = 1933 cm^{-1}). Nevertheless, the $PC^{BIm}P$ ligand possesses weaker π-acceptor properties than the nitrenium-based PNP[47] ligand (ν = 2024 cm^{-1}), which is considered to be a good π acceptor.

Compound **6b** shows very good solubility in CH_3CN, DMSO, dimethylformamide (DMF), acetone, CH_2Cl_2, chloroform, and PO, poor solubility in methanol, Et_2O, isopropyl alcohol, and THF, extremely sparingly solubility in *n*-butanol and other long chain alcohols, and no solubility in benzene, toluene, ethyl acetate, diethyl carbonate, cyclohexanone, diethyl ether, and hydrocarbons.

The thermal stability of $[(PC^{BIm}P)Rh(solvent)][PF_6]$ (**6b**) in solution is mainly determined by its anion stability[90,91] and the ability of the organometallic cationic moiety to react with solvents at elevated temperatures, as we have seen from a number of tests. Thus, a series of experiments was conducted to evaluate the reactivity of **6b** against various substrates. Complex **6b** reacts with chloroform at 25 °C and CH_2Cl_2 at elevated temperatures, giving a range of various reaction products as a consequence of the oxidative addition of halogenated hydrocarbons[56] (Figure S10). Compound **6b** remained stable in CH_3CN under an argon atmosphere by heating to 120 °C over 20 h. A further temperature increase up to 125−130 °C resulted in complete decomposition of the hexafluorophosphate anion and formation of several organometallic products containing the $PC^{BIm}PRh$ fragment (Figure S11). Considering the stability of the PF_6 anion, we observed that hexafluorophosphate was much more stable in basic environments. Thus, its decomposition was not visible in DMF at 150 °C after 17 h and in an *n*-octene/ammonia mixture at 180 °C after 12 h. No rearrangement of the rhodium complex due to $P-C^{Ph}$ bond cleavage was observed through a study of its thermal stability in solution.

The stepwise heating of **6b** in CH_3CN in a dihydrogen (H_2) atmosphere (1 bar) led to the formation of a new organometallic product [39.88 ppm (d, J^{P-Rh} = 157.6 Hz); ^{31}P NMR] followed by slow deposition of rhodium black from solution during prolonged heating at 80 °C. The observed intermediate could not be isolated in the solid state via the fractional crystallization of components from the reaction mixture. Further attempts to obtain classical or nonclassical monometallic $PC^{BIm}PRh$ hydride species through the direct reaction of **6b** with hydrogen in suitable polar solvents were not successful. Nevertheless, the reaction of **6b** with 30 equiv of $KHCO_3$ in THF/H_2O under a H_2 atmosphere proceeds with quantitative conversion to the hydride-bridged dimer $[(PC^{BIm}PRh)_2(\mu\text{-}H)][PF_6]$ (**10**), which is a rare example of a pincer-ligated bimetallic cluster (Scheme 5).[92] It is worth noting that the reaction of complex **6b** with HCOOK also produces **10** in the absence of hydrogen in THF, as revealed by ^{31}P NMR. Such dimerization is evidently favored by insufficient steric hindrance of the phenyl substituents. The μ-hydride characteristic peak appears as a multiplet at −9.15 ppm; the eight protons of the methylene fragments show up as an unresolved multiplet at 4.79 ppm in the ^{1}H NMR spectrum. The ^{31}P NMR spectrum exhibits a doublet at 55.90 ppm (d, J^{P-Rh} = 156.5 Hz) assigned to four phosphorus nuclei along with the typical multiplet of the PF_6 anion. The crystallographic analysis clearly confirms the dinuclear monohydride-bridged structure with a Rh−Rh distance of 2.807 Å and a Rh1−H1−Rh2 bond angle of 109.4(13)° (Figure 7, Table 1). These values give evidence for significant metal−metal interaction in

DOI: 10.1021/acs.inorgchem.5b01428
Inorg. Chem. 2015, 54, 9517−9528

Scheme 5. Formation of Dinuclear Rhodium μ-Hydride Cluster 10 and Hydrogenation of $KHCO_3$ and Preliminary Results of Stoichiometric Decarbonylation of Substrates by 6b

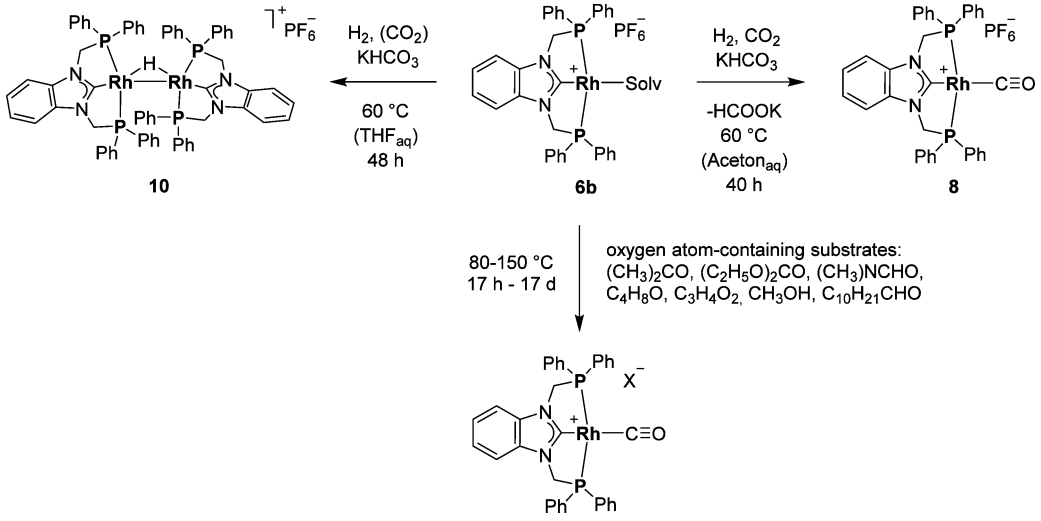

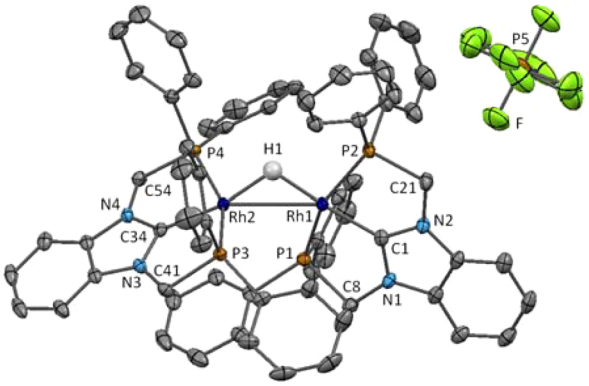

Figure 7. Crystal structure of **10** (50% displacement ellipsoids; hydrogen atoms except H1 were omitted for clarity). Selected interatomic distances (Å) and angles (deg): Rh1−Rh2, 2.8075(2); Rh1−H1, 1.71(2); Rh2−H1, 1.73(2); Rh1−C1, 1.941(2); Rh2−C34, 1.937(2); Rh1−P1, 2.2905(5); Rh1−P2, 2.2379(5); Rh2−P3, 2.2823(5); Rh2−P4, 2.2311(5); N1−C1, 1.363(2); N2−C1, 1.369(3); N3−C34, 1.368(3); N4−C34, 1.367(3); N1−C8, 1.454(3); N2−C21, 1.456(2); N3−C41, 1.452(3); N4−C54, 1.457(3); P1−C8, 1.874(2); P2−C21, 1.867(2); P3−C41, 1.878(2); P4−C54, 1.878(2); Rh1−H1−Rh2, 109.57; Rh2−Rh1−C1, 156.86(6); H1−Rh1−C1, 167.7(8); Rh1−Rh2−C34, 150.23(6); H1−Rh2−C34, 170.7(8); P1−Rh1−P2, 154.36(2); P3−Rh2−P4, 153.88(2).

$[(PC^{BIm}PRh)_2(\mu\text{-}H)][PF_6]$ analogous to a homotypic $[(PC^{m\text{-phenylene}}PPt)_2(\mu\text{-}H)][SbF_6]$ dimer and $[(X(R_3P)_2Pt)_2(\mu\text{-}H)]^+$ clusters, for which the diminution of the Pt−H−Pt angle results in a stronger direct Pt−Pt overlap.[92,93]

Not only is the excision of a carbonyl group from organic substrates considered as an important useful industrial catalytic approach for selective conversion of biorenewable materials or for energy applications,[94,95] but it is also often mentioned as an undesirable reaction, leading to deactivation of an active catalyst through its complexation with a carbonyl group, for instance, in catalytic dehydrogenation.[95−98] The activity of transition-metal pincer complexes in stoichiometric CO excision through C−H and C−C bond activation is pronounced and is reflected in numerous studies on $[(PNP)RuH_2(H)]$,[99] $[(PC^{m\text{-phenylene}}P)\text{-}IrH_2]$,[29] $[(^{CF_3}PC^{m\text{-phenylene}}P^{CF_3})Ir(L)]$,[98] $[(PC^{m\text{-phenylene}}P)\text{-}RhN_2]$,[100] $[(PN^{Py}P)RhH(C_6H_5)][PF_6]$,[97] and $[(PBP)Rh]$.[45,46] Therefore, we were interested in the reactivity of **6b** against oxygen-containing substrates at elevated temperatures. According to the ^{31}P NMR screening experiments, heating of **6b** in β-propiolactone, THF, diethyl carbonate, DMF, acetone, methanol and aliphatic aldehydes (Figures S14−S21) ultimately results in C−H or C−C bond activation followed by formation of the $[(PC^{BIm}P)Rh^{I}CO]$ moiety. Such thermally induced decarbonylation is accompanied in most cases by degradation of the PF_6 anion in neutral environments. The ^{31}P NMR monitoring of the reaction with undecanal exemplarily shows a slow transformation of **6b** to the carbonyl complex at 110 °C, while no formation of intermediary organometallics could be observed. The further development of this system, allowing regeneration of active $[PC^{BIm}PRh(I)]$ species by CO dissociation from the complex, would open up applications in catalytic defunctionalization of organic compounds.

We also tested the catalytic hydrogenation of CO_2 (10−30 bar) and $KHCO_3$ with H_2 (10 bar) in THF/H_2O and acetone/H_2O solvent mixtures at 60 °C for 40 h. Complex **6b** produced potassium formate with very low catalytic activity in acetone/H_2O under such mild reaction conditions. No detectable decomposition of either $[PC^{BIm}PRh(L)]$ or $[PF_6]$ was observed under a reducing atmosphere of H_2 in a basic environment. It is worth noting that **6b** has been converted quantitatively into **8** in an acetone/H_2O mixture during the reaction, as was confirmed by ^{31}P NMR analysis (Figure S24). A small amount of formed carbonyl complex **8** was also identified in ^{31}P NMR after the reaction of CO_2 and H_2 without the addition of $KHCO_3$. The use of the rhodium carbonyl complex **8** under the same hydrogenation conditions led again to conversion of potassium bicarbonate to potassium formate. Therefore, $[PC^{BIm}PRhCO][PF_6]$ can be seen as a resting state of the catalytic active species. Unfortunately, we could not find any traces of free CO in the gas phase over the reaction mixture using micro GC−MS and IR techniques (Figures S27 and S28). It follows that decarbonylation of bicarbonate in aqueous acetone occurs stoichiometrically on complex **6b**, in accordance with observations made by Ozerov et al.[99] (Scheme 5).

DOI: 10.1021/acs.inorgchem.5b01428
Inorg. Chem. 2015, 54, 9517−9528

Table 1. Crystallographic Data for Compounds 5, 6b, 7, 8, and 10

	5	6b	7	8	10
formula	$C_{33}H_{29}F_6N_2P_3$	$C_{39}H_{37}F_6N_5P_3Rh$	$C_{33}H_{28}ClF_6N_2P_3Pd$	$C_{34}H_{28}F_6N_2OP_3Rh$	$C_{70}H_{67}F_6N_4OP_5Rh_2$
fw	660.49	885.56	801.33	790.40	1454.92
color/habit	yellow/fragment	red-brown/fragment	yellow/plate	yellow/fragment	orange/fragment
cryst dimens, mm^3	0.45 × 0.50 × 0.65	0.17 × 0.23 × 0.28	0.13 × 0.36 × 0.48	0.13 × 0.15 × 0.51	0.16 × 0.19 × 0.27
cryst syst	triclinic	monoclinic	triclinic	triclinic	triclinic
space group	$P\bar{1}$	$P\,2_1/n$	$P\bar{1}$	$P\bar{1}$	$P\bar{1}$
a, Å	13.1758(5)	10.2501(7)	13.8424(6)	11.0952(5)	12.0213(3)
b, Å	13.3209(5)	18.5633(13)	15.2793(7)	11.8453(5)	15.1548(4)
c, Å	18.7343(6)	20.8712(14)	15.9485(7)	12.5833(6)	18.3327(5)
α, deg	75.565(2)	90	86.477(2)	99.828(2)	99.852(2)
β, deg	72.988(1)	101.726(3)	89.297(2)	94.714(2)	103.228(1)
γ, deg	82.484(2)	90	76.105(2)	94.948(2)	94.338(1)
V, $Å^3$	3039.04(19)	3888.4(5)	3268.2(3)	1615.50(13)	3180.27(15)
Z	4	4	4	2	2
T, K	123	123	123	123	123
D_{calcd}, g cm^{-3}	1.444	1.513	1.629	1.625	1.519
μ, mm^{-1}	0.260	0.627	0.858	0.744	0.710
$F(000)$	1360	1800	1608	796	1484
θ range, deg	2.33−25.34	1.48−25.37	1.38−25.46	1.65−25.39	2.32−31.45
index ranges (h, k, l)	±15, ±16, ±22	±12, ±22, ±25	±16, ±18, ±19	±13, ±14, ±15	±15, ±18, ±22
no. of rflns collected	142753	89396	114337	45951	82566
no. of indep rflns/R_{int}	11192/0.0362	7110/0.0428	12112/0.0200	5924/0.0287	12981/0.0443
no. of obsd rflns [$I > 2\sigma(I)$]	9671	6269	11308	5778	11336
no. of data/restraints/param	11192/0/793	7110/0/ 490	12112/0/829	5924/0/424	12981/13/868
R1/wR2 [$I > 2\sigma(I)$][a]	0.0294/0.0725	0.0377/0.0973	0.0189/0.0504	0.0180/0.0466	0.0257/0.0595
R1/wR2 (all data)[a]	0.0366/0.0764	0.0451/0.1053	0.0208/0.0514	0.0186/0.0470	0.0329/0.0621
GOF (on F^2)[a]	1.042	1.077	1.051	1.056	1.035
largest diff peak/hole (e $Å^{-3}$)	0.047/−0.342	1.940/−1.055	0.348/−0.313	0.442/−0.203	0.597/−0.553

[a] $R1 = \sum(||F_o| - |F_c||)/\sum|F_o|$; $wR2 = \{\sum[w(F_o^2 - F_c^2)^2]/\sum[w(F_o^2)^2]\}^{1/2}$; $GOF = \{\sum[w(F_o^2 - F_c^2)^2]/(n-p)\}^{1/2}$.

APPLICATION OF [$PC^{BIM}PRH(L)$][PF_6] IN HYDROBORATION

In order to evaluate the catalytic activity of **6b**, we used borylation as a test reaction. In general, transition-metal-catalyzed hydroboration can be run through different mechanistic pathways.[101] Depending on the particular catalysts used, various target regio- and stereoselective products can be achieved. This assertion is demonstrably illustrated by a number of peculiar borylation approaches, such as the synthesis of (*Z*)-vinylboronates promoted by [$(PN^{Py}P)RuH_2(H)_2$],[102] dehydrogenative alkene borylation to (*E*)-vinylboronates using [(PSiP)Pd][OTf][103] or dehydrogenative alkyne borylation with [$(SiNN)IrH(HBPin)_2$],[104] [$(NNN)CoCH_3$]-catalyzed enantioselective hydroboration of alkenes,[105] and alkene isomerization−hydroboration.[106]

We have performed borylation with phenylacetylene and pinacolborane (HBPin) as a model reaction according to a common procedure. No reaction was observed between HBPin and phenylacetylene in THF at room temperature and 60 °C within 24 h in the absence of the rhodium complex **6b**. After the addition of **6b**, hydroboration proceeds catalytically with the selective formation of β-(*E*)-vinylboronate (88%, GC−MS). Besides the main product, β-(*Z*)-vinylboronate and α-vinylboronate along with hydrogenated α- and β-alkylboronates were identified in the GC−MS chromatogram and ^{1}H NMR spectra (Figures S30−S32 and S34). The reaction occurs until full consumption of phenylacetylene within less than 17 h (Scheme 6).

The predominant generation of a β-*E* isomer proves that transformation on the rhodium center is controlled by steric influence. However, the 1,2-H migration, followed by η^1-Rh-vinylidene formation, leading to β-(*Z*)-vinylboronate as the minor product, apparently also takes place but is not prevalent in this case.[102,107,108] ^{31}P NMR spectra recorded after 2 and 31 h reveal the presence of **6b**, a new species with an intense characteristic doublet at 43.67 ppm (J^{Rh-P} = 157.9 Hz), and the previously described dimer **10** (Figure S33).

Scheme 6. *E*-Selective Hydroboration of Phenylacetylene with Pinacolborane Using 6b[a]

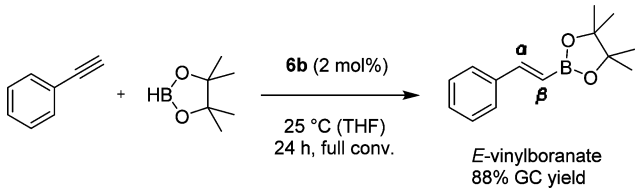

[a] Conversions are estimated by ^{1}H NMR and GC−MS techniques.

In summary, we have developed a gram-scale synthesis of a benzimidazolium-based pincer ligand precursor. The new [5,5]-membered carbene-centered $PC^{BIm}PRh^I$ and -Pd^{II} complexes were synthesized and fully characterized using NMR, IR, MS, and X-ray techniques. The thermal stability and reactivity of $PC^{BIm}PRh^I$ complexes were assessed in both the solid state and solution. On the basis of the studied stoichiometric and catalytic transformations, it was clearly shown that the $PC^{BIm}P$-ligated rhodium(I) complex basically tends to decarbonylate the oxygen-containing substrates. The observations that we made on a range of reactions indicate that $PC^{BIm}PRh^I$ undergoes two main conversion pathways, forming more

DOI: 10.1021/acs.inorgchem.5b01428
Inorg. Chem. 2015, 54, 9517−9528

thermodynamically stable species: a carbonyl complex and a hydride-containing dimer. We report herein the synthesis and single-crystal X-ray structural analysis of a dinuclear μ-hydride rhodium cluster. Additionally, it was found that $PC^{BIm}PRh^{I}$ catalyzes the B−H addition on the triple bond of phenylacetylene, selectively leading to (*E*)-vinylboronate through a conventional cis-hydroboration pathway. Further applications of $PC^{BIm}P$-based organometallics in promising catalytic transformations are currently in progress.

EXPERIMENTAL SECTION

All reactions were carried out under an argon atmosphere, unless noted. Chemicals were purchased from Acros Organics, ABCR, or Sigma-Aldrich and used as received, unless otherwise specified. Glassware was heated and dried under vacuum prior to use. Tetrahydrofuran (THF), diethyl ether, toluene, and pentane were purified by passing through a MBraun SPS-800 solvent purification system. Isopropyl alcohol, CH_3CN, methanol, acetone, chloroform, CH_2Cl_2, and other solvents were dried over 3 Å molecular sieves. The ^{1}H, ^{19}F, ^{13}C, and ^{31}P NMR spectra were recorded on AV-300, AV-360, and AV-500C MHz Bruker spectrometers. Spectroscopic chemical shifts were referenced to the residual proton signal of the deuterated solvents for ^{1}H and ^{13}C NMR spectra. ^{31}P NMR spectra were calibrated to a 85% H_3PO_4 standard solution (internal capillary). Deuterated solvents were purchased from Deutero or Eurisotop and dried over 3 Å molecular sieves. Multiplicity is denoted using the following abbreviations: s, singlet; d, doublet; t, triplet; q, quartet; m, multiplet. Assignment of the signals was based on one-dimensional and two-dimensional COSY, HMBC, and HSQC NMR techniques. EA was measured at the Laboratory for Microanalysis at the Institute of Inorganic Chemistry at Technische Universität München. Electrospray ionization mass spectrometry (ESI MS) analysis was performed on a Varian 500-MS spectrometer in the positive-ionization mode using undegassed methanol, isopropyl alcohol, THF, or CH_3CN. IR spectra were recorded on a Bruker Vertex 70 spectrometer with a Bruker Platinum ATR setup and an integrated MCT detector. Samples for IR measurements were used in the solid state. For GC analysis, a Varian Saturn 2100T GC MS chromatograph with a 30 m Agilent GC column (P/N: CP8944) and a Varian 490-Micro GC-TCD system (Column 492001450 COX 1m, heated, helium carrier gas, 80 °C) were used. TGA was measured on a TGAQ5000 analyzer from TA Instruments (Waters).

Single-Crystal XRD. Data were collected on a single-crystal X-ray diffractometer equipped with a CCD detector (APEX II, κ-CCD), a fine-focused sealed tube with Mo Kα radiation (λ = 0.71073 Å) and a graphite monochromator or a FR591 rotating anode with Mo Kα radiation and a Montel optic, by using the *APEX2* software package.[109] The measurements were performed on single crystals coated with perfluorinated ether. The crystals were fixed on the top of a glass fiber and transferred to the diffractometer. Crystals were frozen under a stream of cold nitrogen. A matrix scan was used to determine the initial lattice parameters. Reflections were merged and corrected for Lorenz and polarization effects, scan speed, and background using *SAINT*.[110] Absorption corrections, including odd and even ordered spherical harmonics, were performed using *SADABS*.[110] Space group assignments were based upon systematic absences, E statistics, and successful refinement of the structures. Structures were solved by direct methods with the aid of successive difference Fourier maps[111] and refined against all data using *APEX 2* software[109] in conjunction with *SHELXL-97* or *SHELXL2014*[112] and *SHELXLE*.[113] Methyl hydrogen atoms were refined as part of rigid rotating groups, with a C−H distance of 0.98 Å and $U_{iso}(H) = 1.5U_{eq}(C)$. Other hydrogen atoms were placed in calculated positions and refined using a riding model, with methylene and aromatic C−H distances of 0.99 and 0.95 Å, respectively, and $U_{iso}(H) = 1.2U_{eq}(C)$. If not mentioned otherwise, non-hydrogen atoms were refined with anisotropic displacement parameters. Full-matrix least-squares refinements were carried out by minimizing $\sum w(F_o^2 - F_c^2)^2$ with a *SHELXL-97*[112] weighting scheme. Neutral atom scattering factors for all atoms and anomalous dispersion corrections for the non-hydrogen atoms were taken from *International Tables for Crystallography*.[114] Images of the crystal structures were generated by *PLATON*.[115] Crystallographic data for structures **5**, **6a**, **6b**, **7**, **8**, and **10** (Table 1) have also been deposited with the Cambridge Crystallographic Data Centre (CCDC 1405697−1405702). These coordinates can be obtained, upon request, from the Director, Cambridge Crystallographic Data Centre, 12 Union Road, Cambridge CB2 1EZ, U.K. [fax (+44)1223-336-033; e-mail deposit@ccdc.cam.ac.uk].

1-[(Diphenylphosphoryl)methylene]benzimidazole (2). A round-bottomed flask was charged with benzimidazole (1.20 g, 10.0 mmol, 1.00 equiv), [(diphenylphosphoryl)methylene]-4-methylbenzenesulfonate (**1**; 4.02 g, 10.0 mmol, 1.00 equiv), and potassium carbonate (9.67 g, 70.0 mmol, 7.00 equiv) under an air atmosphere. After the addition of 40 mL of DMSO, the suspension was intensively stirred at 90 °C for 24 h. The reaction mixture was cooled to 50 °C, and DMSO was removed under reduced pressure. The crude product was isolated by extraction with $CHCl_3/H_2O$ and evaporation of the organic phase. A final washing of the residue with diethyl ether and drying in a vacuum give colorless solid product **2** (3.25 g, 97%). Anal. Calcd for $C_{20}H_{17}N_2OP$: C, 72.28; H, 5.16; N, 8.43; P, 9.32. Found: C, 71.88; H, 5.12; N, 8.08; P, 9.15. ^{1}H NMR ($CDCl_3$, 360 MHz): δ 7.86 (s, 1H), 7.67 (m, 5H), 7.50 (td, J = 7.4 and 1.5 Hz, 2H), 7.39 (td, J = 7.7 and 3.0 Hz, 4H), 7.15 (m, 3H), 4.92 (d, J = 5.9 Hz, 2H). ^{13}C NMR ($CDCl_3$, 90 MHz): δ 143.20 (s, 1C), 142.94 (s, 1C), 134.10 (s, 1C), 132.92 (d, J = 2.74 Hz, 2C), 131.17 (d, J = 9.51 Hz, 4C), 129.29 (d, J = 100.35 Hz, 2C), 129.05 (d, J = 11.91 Hz, 4C), 123.22 (s, 1C), 122.33 (s, 1C), 120.21 (s, 1C), 109.76 (s, 1C), 45.73 (d, J = 73.45 Hz, 1C). ^{31}P NMR ($CDCl_3$, 146 MHz): δ 25.58 (s, 1 P). ESI MS: m/z 333.0 ($[C_{20}H_{18}N_2OP]^+$, $[C^{BIm}PO + H]^+$).

1,3-Bis[(diphenylphosphoryl)methylene]benzimidazolium 4-Methylbenzylsulfonate (3). **2** (1.45 g, 4.3 mmol, 1.00 equiv) and **1** (3.04 g, 7.7 mmol, 1.80 equiv) were ground by stirring under vacuum for 1 h. Thereafter, the flask was backfilled with argon and stirred at 145 °C for 12 h. After the reaction was completed, the solid material was dissolved in CH_2Cl_2, and the product was precipitated from the solution by the addition of toluene, filtered, and dried in vacuo. The second product portion was obtained by evaporation of CH_2Cl_2 and multiple extractions of byproducts from the solid crude substance with toluene over prolonged time. Further, the product can be worked up by extraction with a warm H_2O/toluene (3:1) mixture. After water was removed, the residue was redissolved in $CHCl_3$ or CH_2Cl_2 and dried over sodium sulfate. The product (2.87 g, 93%) was obtained after evaporation of the organic phase as a colorless solid material. Anal. Calcd for $C_{39}H_{34}N_2O_5P_2S$: C, 66.47; H, 4.86; N, 3.98; O, 11.35; P, 8.79; S, 4.55. Found: C, 66.59; H, 5.11; N, 3.73; P, 8.62; S, 4.67. ^{1}H NMR ($CDCl_3$, 360 MHz): δ 10.69 (s, 1H), 8.14 (m, 2H), 7.91 (m, 10H), 7.55 (m, 2H), 7.48 (m, 4H), 7.40 (m, 8H), 7.22 (d, J = 8.0 Hz, 2H), 5.43 (d, J = 5.9 Hz, 4H), 2.37 (s, 3H). ^{13}C NMR ($CDCl_3$, 90 MHz): δ 144.03 (s, 1C), 143.01 (s, 1C), 140.09 (s, 1C), 133.21 (d, J = 2.6 Hz, 4C), 131.63 (s, 2C), 133.38 (d, J = 10.0 Hz, 8C), 129.37 (d, J = 12.5 Hz, 8C), 128.97 (s, 2C), 127.87 (d, J = 103.0 Hz, 4C), 127.63 (s, 2C), 126.14 (s, 2C), 115.2 (s, 2C), 48.18 (d, J = 67.2 Hz, 2C), 21.52 (s, 1C). ^{31}P NMR ($CDCl_3$, 146 MHz): δ 26.24 (s, 2P). ESI MS m/z: 547.1 ($[C_{33}H_{29}N_2O_2P_2]^+$, $[OPC^{BIm}PO]^+$).

1,3-Bis(diphenylphosphinomethylene)benzimidazoline (4). To a suspension of **3** (1.30 g, 1.8 mmol, 1.00 equiv) in chlorobenzene (60 mL) were added poly(methylhydrosiloxane) (1.83 g, 4.4 mmol, 2.50 equiv; M_n = 390 g mol^{-1}) and titanium(IV) isopropoxide (1.9 mL, 6.2 mmol, 3.60 equiv) under argon. The reaction mixture was stirred for 2 h at 70 °C. After conversion was complete (^{31}P NMR monitoring is necessary), the mixture was cooled to 25 °C, and all volatiles were removed in vacuo. After pentane was added to the residue, the suspension formed was stirred for over 3 h and filtered via cannula. Additionally, the crude product was washed three times with a small amount of degassed cold pentane, dissolved in diethyl ether, filtered, and recrystallized from a concentrated diethyl ether solution at −40 °C. A total of 740.0 mg (82%) of colorless **4** was isolated. Anal. Calcd for $C_{33}H_{30}N_2P_2$: C, 76.73; H, 5.85; N, 5.42; P, 11.99. Found: C,

DOI: 10.1021/acs.inorgchem.5b01428
Inorg. Chem. 2015, 54, 9517−9528

77.24; H, 5.92; N, 5.45; P, 11.62. ^{1}H NMR ($CDCl_3$, 500 MHz): δ 7.46 (m, 8H), 7.34 (m, 12H), 6.61 (m, 2H), 6.41 (m, 2H), 4.66 (s, 2H), 3.81 (d, J = 5.52 Hz, 4H). ^{13}C NMR ($CDCl_3$, 76 MHz): δ 142.14 (d, J = 4.77 Hz, 2C), 137.32 (d, J = 12.79 Hz, 4C), 132.99 (d, J = 18.10 Hz, 8C), 129.08 (s, 4C), 128.74 (d, J = 6.60 Hz, 8C), 119.18 (s, 2C), 106.27 (s, 2C), 77.98 (t, J = 7.02 Hz, 1C), 50.73 (d, J = 7.69 Hz, 2C). ^{31}P NMR ($CDCl_3$, 146 MHz): δ −25.00 (s, 2P).

1,3-Bis(diphenylphosphinomethylene)benzimidazolium Hexafluorophosphate (5). To a colorless solution of **4** (710.0 mg, 1.35 mmol, 1.00 equiv) in 17 mL of degassed dry THF cooled to −78 °C was added in one portion triphenylcarbenium hexafluorophosphate (510.0 mg, 1.31 mmol, 0.97 equiv). The mixture was stirred for 30 min with warming to room temperature. After the reaction was complete, the amount of THF was reduced in vacuo, and the product was precipitated by the addition of 15 mL of degassed dry toluene. The formed suspension was stirred overnight at room temperature and filtered via cannula. The crude solid product was then redissolved in THF, filtered through a syringe filter, and precipitated by the addition of diethyl ether. Recrystallization of the precipitate from THF/Et_2O (2:8) at −40 °C yielded 790.0 mg (86%) of pure colorless crystalline material **5**. Anal. Calcd for $C_{33}H_{29}F_6N_2P_3$: C, 60.01; H, 4.43; F, 17.26; N, 4.24; P, 14.07. Found: C, 60.31; H, 4.62; N, 4.38; P, 14.06. ^{1}H NMR (CD_3CN, 500 MHz): δ 8.69 (s, 1H), 7.67 (m, 2H), 7.53 (m, 2H), 7.41 (m, 20H), 5.15 (d, J = 5.35 Hz, 4H). ^{13}C NMR (CD_3CN, 126 MHz): δ 140.61 (t, J = 3.91 Hz, 1C), 134.47 (d, J = 12.27 Hz, 4C), 133.91 (d, J = 19.87 Hz, 8C), 132.30 (s, 2C), 131.24 (s, 4C), 130.13 (d, J = 7.18 Hz, 8C), 127.90 (s, 2C), 114.76 (s, 2C), 47.55 (d, J = 20.95 Hz, 2C). ^{31}P NMR (CD_3CN, 202 MHz): δ −14.05 (s, 2P), −144.00 (sept, J = 706.71 Hz, 1P). ^{19}F NMR (CD_3CN, 471 MHz): δ −72.80 (d, J = 706.82 Hz, 6F).

1,3-Bis(diphenylphosphinomethylene)benzimidazol-2-ylrhodium Acetonitrile/Dimethyl Sulfoxide Hexafluorophosphate (6). **5** (480.0 mg, 0.7 mmol, 1.00 equiv) was added to the solution of $[\mu$-$OCH_3Rh(COD)]_2$ (170.0 mg, 0.35 mmol, 0.50 equiv) in 10 mL of degassed THF at room temperature and stirred for 17 h. After the reaction was complete, all volatiles were removed in vacuo. The formed amorphous solid was then redissolved in DMSO (for **6a**) or in CH_3CN (for **6b**) and stirred for 3 h under a H_2 atmosphere (0.5 bar over the atmospheric pressure). The reaction mixture was filtered through a 0.20 μm syringe filter, and the solvent was partially reduced in vacuo. The yellow needle-shaped crystals of substance **6a** (450.0 mg, 76%) were obtained by the addition of diethyl ether after 10 days. The yellow crystals of substance **6b** (340.0 mg 61%) were obtained by the addition of diethyl ether. **6a**. ^{1}H NMR ($(CD_3)_2SO$, 300 MHz): δ 7.89 (m, 8H), 7.60 (m, 14H), 7.41 (m, 2H), 5.32 (m, 4H). ^{31}P NMR ($(CD_3)_2SO$, 203 MHz): δ 48.23 (d, J = 151.08 Hz, 2P), −144.00 (sept, J = 711.40 Hz, 1P). **6b**. Anal. Calcd for $C_{35}H_{31}F_6N_3P_3Rh$ (+0.20 equiv of C_2H_3N): C, 53.46; H, 4.00; F, 14.33; N, 5.63; P, 11.68; Rh, 12.94. Found: C, 53.44; H, 4.85; N, 5.24; P, 11.51. ^{1}H NMR (CD_3CN, 360 MHz): δ 7.80 (m, 8H), 7.54 (m, 12H), 7.40 (m, 2H), 7.30 (m, 2H), 4.97 (vt, J = 3.04 Hz, 4H). ^{13}C NMR (CD_3CN, 126 MHz): δ 198.96 (dt, J = 51.2 and 11.9 Hz, 1C), 134.93 (t, J = 6.0 Hz, 2C), 134.25 (t, J = 20.0 Hz, 4C), 133.76 (vt, J = 7.7 Hz, 8C), 131.97 (s, 4C), 130.13 (vt, J = 4.9 Hz, 8C), 124.39 (s, 2C), 111.97 (s, 2C), 51.43 (vt, J = 16.77 Hz, 2C). ^{31}P NMR (CD_3CN, 146 MHz): δ 45.84 (d, J = 152.79 Hz, 2P), −144.00 (sept, J = 706.37 Hz, 1P). ^{19}F NMR (CD_3CN, 235 MHz): δ −72.86 (d, J = 706.26 Hz, 6F). ESI MS: m/z 585.6 ($[C_{33}H_{28}KN_2O_2P_2]^+$, $[OPC^{BIm}POK]^+$), 617.5 ($[C_{33}H_{28}N_2P_2Rh]^+$, $[PC^{BIm}PRh]^+$), 633.4 ($[C_{33}H_{28}N_2OP_2Rh]^+$, $[PC^{BIm}PORh]^+$), 649.4 ($[C_{33}H_{28}N_2O_2P_2Rh]^+$, $[OPC^{BIm}PORh]^+$).

1,3-Bis(diphenylphosphinomethylene)benzimidazol-2-ylpalladium Chloride Hexafluorophosphate (7). **5** (104.3 mg, 0.15 mmol, 1.00 equiv) was added portionwise to a suspension of $PdCl_2$ (26.9 mg, 0.15 mmol, 1.00 equiv) in 10 mL of degassed dry DMF at room temperature and stirred for 8 h at 60 °C. After the reaction was complete, all volatiles were removed in vacuo. The formed amorphous solid was then redissolved in CH_3CN and filtered. The colorless fine-crystalline compound **7** (41.0 mg, 34%) was obtained after crystallization from a CH_3CN/Et_2O mixture. Anal. Calcd for $C_{33}H_{28}ClF_6N_2P_3Pd$: C, 49.46; H, 3.52; Cl, 4.42; F, 14.22; N, 3.50; P, 11.60; Pd, 13.28. Found: C, 49.17; H, 3.75; N, 3.57; P, 11.30. ^{1}H NMR (CD_3CN, 500 MHz): δ 7.99 (m, 8H), 7.71 (m, 2H), 7.67 (m, 4H), 7.61 (m, 8H), 7.58 (m, 2H), 5.45 (vt, J = 3.34 Hz, 4H). ^{13}C NMR (CD_3CN, 126 MHz): δ 178.82 (t, J = 5.78 Hz, 1C), 134.37 (vt, J = 7.31 Hz, 8C), 134.15 (t, J = 6.36 Hz, 2C), 133.68 (s, 4C), 130.53 (vt, J = 5.77 Hz, 8C), 127.99 (t, J = 25.22 Hz, 4C), 126.63 (s, 2C), 114.20 (s, 2C), 52.43 (vt, J = 17.67 Hz, 2C). ^{31}P NMR (CD_3CN, 203 MHz): δ 38.16 (s, 2P), −144.00 (sept, J = 706.89 Hz, 1P). ^{19}F NMR (CD_3CN, 235 MHz): δ −72.89 (d, J = 706.26 Hz, 6F). ESI MS: m/z 647.3 ($[C_{66}H_{57}ClN_4OP_4Pd_2]^{2+}$, $[(PC^{BIm}P)_2Pd_2Cl(OH)]^{2+}$), 656.2 ($[C_{33}H_{28}ClN_2P_2Pd]^+$, $[PC^{BIm}PPdCl]^+$). FAB MS: m/z 655.4 ($[C_{33}H_{28}ClN_2P_2Pd]^+$, $[PC^{BIm}PPdCl]^+$). HRMS. Calcd: m/z 655.04456. Found: m/z 655.04491 ($[C_{33}H_{28}ClN_2P_2Pd]^+$, $[PC^{BIm}PPdCl]^+$).

1,3-Bis(diphenylphosphinomethylene)benzimidazol-2-ylrhodium Carbonyl Hexafluorophosphate (8). A solution of 1,3-bis(diphenylphosphinomethylene)benzimidazol-2-ylrhodium acetonitrile hexafluorophosphate (**6b**; 23.0 mg, 0.03 mmol, 1.00 equiv) in 0.5 mL of PO was pressurized with 2 bar of ^{13}CO in a Young valve NMR tube. After 2 h, the tube containing the reaction mixture was flushed with degassed diethyl ether. Crystallization gave 20.0 mg (98%) of **8** in the form of light-yellow needles. Anal. Calcd for $C_{34}H_{28}F_6N_2OP_3Rh$: C, 51.66; H, 3.57; F, 14.42; N, 3.54; O, 2.02; P, 11.76; Rh, 13.02. Found: C, 51.28; H, 4.02; N, 3.21; P, 11.36. ^{1}H NMR (CD_3CN, 300 MHz): δ 7.82 (m, 8H), 7.65 (m, 2H), 7.59 (dq, J = 14.30 and 7.27 Hz, 12H), 7.50 (m, 2H), 5.37 (vt, J = 3.14 Hz, 4H). ^{13}C NMR (CD_3CN, 126 MHz): δ 197.21 (dt, J = 40.48 and 12.63 Hz, 1C), 195.96 (s, 1C), 134.71 (vt, J = 5.69 Hz, 2C), 134.00 (vt, J = 7.59 Hz, 8C), 132.90 (s, 4C), 132.01 (vt, J = 23.45 Hz, 4C), 130.45 (vt, J = 5.48 Hz, 8C), 126.09 (s, 2C), 125.74 (s, C, free CO), 113.85 (s, 2C), 54.31 (vt, J = 17.61 Hz, 2C). ^{31}P NMR (CD_3CN, 203 MHz): δ 55.41 (d, J = 138.49 Hz, 2P), −144.00 (sept, J = 707.27 Hz, 1P). ^{19}F NMR (CD_3CN, 471 MHz): δ −72.60 (d, J = 706.73 Hz, 6F). ESI MS. m/z 617.4 ($[C_{33}H_{28}N_2P_2Rh]^+$, $[PC^{BIm}PRh]^+$), 633.3 ($[C_{33}H_{28}N_2OP_2Rh]^+$, $[PC^{BIm}PORh]^+$), 645.4 ($[C_{34}H_{28}N_2OP_2Rh]^+$, $[PC^{BIm}PRhCO]^+$), 649.3 ($[C_{33}H_{28}N_2O_2P_2Rh]^+$, $[OPC^{BIm}PORh]^+$). IR: ν_{C-O} 1995.34 cm^{-1}.

1,3-Bis(diphenylphosphinomethylene)benzimidazol-2-ylrhodium Ethylene Hexafluorophosphate (9). The ethylene gas was introduced to the solution of **6b** in a Young NMR tube. Subsequently, the color of the mixture changed slightly to a maize yellow; after 2 h, the ^{31}P NMR spectra were recorded. Reaction of **6b** with ethylene leads to the reversible formation of **9** in PO, CH_2Cl_2, and THF solutions at 25 °C. In all cases, the removal of volatile components led to the formation of **6b**, and complex **9** could not be isolated. Crystallization directly from the reaction mixture did not give the crystalline product **9**.

Bis[1,3-bis(diphenylphosphinomethylene)benzimidazol-2-ylrhodium] μ-Hydride Hexafluorophosphate (10). **6b** (17.4 mg, 0.02 mmol, 1.00 equiv) was added to a biphasic solution of $KHCO_3$ (62.6 mg, 0.62 mmol, 30.00 equiv) in 0.75 mL of degassed water and 3.5 mL of degassed THF. The autoclave was pressurized with 10 bar of H_2 and 30 bar of CO_2 and thermostated at 60 °C. After 48 h, all volatiles were removed in vacuo. The product was then redissolved in acetone and filtered via a syringe filter. After the addition of diethyl ether to an acetone solution, filtration, and drying of precipitate, the terra-cotta-colored amorphous compound **10** (27.4 mg, 96%) was obtained. Anal. Calcd for $C_{66}H_{57}F_6N_4P_5Rh_2$ (+1.00 equiv of $C_4H_{10}O$): C, 57.78; H, 4.64; F, 7.83; N, 3.85; O, 1.10; P, 10.64; Rh, 14.15. Found: C, 57.39; H, 5.06; N, 3.49; P, 10.27. Compound **10** can also be synthesized by stirring of **6b** in a THF suspension containing excess HCOOK within 24 h at 25 °C under an argon atmosphere. ^{1}H NMR ($(CD_3)_2CO$, 360 MHz): δ 7.68 (m, 16H), 7.49 (m, 4H), 7.32 (m, 4H), 7.24 (vt, J = 7.39 Hz, 8H), 7.07 (vt, J = 7.56 Hz, 16H), 4.79 (s, 8H), −9.15 (m, 1H). ^{31}P NMR ($(CD_3)_2CO$, 146 MHz): δ 55.90 (d, J = 156.48 Hz, 4P), −144.00 (sept, J = 706.89 Hz, 1P).

Thermal Stability in Solutions. The thermal stability and reactivity of the rhodium complex **6b** in various solvents were assessed according to the following procedure: **6b** (3−7 mg) was dissolved in 0.45 mL of a degassed solvent in a NMR tube at room temperature in a glovebox. The NMR tube was placed in an oil bath;

DOI: 10.1021/acs.inorgchem.5b01428
Inorg. Chem. 2015, 54, 9517−9528

the tube contents was heated up to a certain temperature, cured at this temperature over a definite period, and analyzed using NMR techniques. After the measurements, the NMR tube was placed back in the oil bath again and the procedure was repeated, reaching another higher temperature limit. Reaction of **6b** with hydrogen was performed in a Young NMR tube.

CO_2 Hydrogenation and Decarbonylation of an Acetone/Bicarbonate Mixture. A solution of $KHCO_3$ (25.3 mg, 0.25 mmol, 100.00 equiv) in 0.5 mL of H_2O and 1.5 mL of organic solvent (THF or acetone) was added to a stainless steel 25 mL high-pressure autoclave containing complex **6b** (2.1 mg, 2.50 μmol, 1.00 equiv) and equipped with a magnetic stirring bar. Then the reactor was pressurized with H_2 (10 bar) and CO_2 (10−30 bar) and thermostated at 60 °C. After stirring for 40 h, the vessel was cooled and the excess gases vented. The reaction mixture was analyzed using micro GC-TCD and NMR.

Hydroboration Procedure for 2-[(*E*)-2-Phenylethenyl]-4,4,5,5-tetramethyl-1,3,2-dioxaborolane. In a glovebox, phenylacetylene (7.8 μL, 0.07 mmol, 1.00 equiv) and pinacolborane (12.6 μL, 0.08 mmol, 1.20 equiv) were dissolved in 0.45 mL of degassed THF-d_8 in an NMR tube. After the addition of **6b** (1.1 mg, 1.40 μmol, 0.02 equiv) to the prepared solution, the NMR tube was shaken and placed in an NMR spectrometer. Subsequently, the reaction mixture was analyzed by GC−MS. The reaction was reproduced at least three times.

■ ASSOCIATED CONTENT

Supporting Information

The Supporting Information is available free of charge on the ACS Publications website at DOI: 10.1021/acs.inorgchem.5b01428.

All experimental procedures and obtained analytical data of new compounds (NMR, MS, IR, TGA, and EA) (PDF)

Single-crystal X-ray structure information for **6a**, **6b**, and **7**−**10** in CIF format (CIF)

■ AUTHOR INFORMATION

Corresponding Author

*E-mail: rieger@tum.de. Tel: +49-89-289-13570. Fax: +49-89-289-13562.

Notes

The authors declare no competing financial interest.

■ ACKNOWLEDGMENTS

The authors thank Drs. Sergej Vagin, Dante Castillo, and Stephan Salzinger for valuable discussions. Andriy Plikhta is grateful for a generous scholarship from the Konrad-Adenauer Foundation.

■ REFERENCES

(1) Diez-Gonzalez, S.; Marion, N.; Nolan, S. P. *Chem. Rev. (Washington, DC, U. S.)* **2009**, *109* (8), 3612−3676.
(2) Scholl, M.; Ding, S.; Lee, C. W.; Grubbs, R. H. *Org. Lett.* **1999**, *1* (6), 953−956.
(3) Herrmann, W. A. *Angew. Chem., Int. Ed.* **2002**, *41* (8), 1290−1309.
(4) Casin, C. S. J. *N-Heterocyclic Carbenes in Transition Metal Catalysis and Organocatalysis*; Springer: Dordrecht, The Netherlands, 2011; p 340.
(5) Díez-González, S. *N-Heterocyclic Carbenes. From Laboratory Curiosities to Efficient Synthetic Tools*; Royal Society of Chemistry: London, 2010; p 442.
(6) Schaper, L.-A.; Hock, S. J.; Herrmann, W. A.; Kühn, F. E. *Angew. Chem., Int. Ed.* **2013**, *52* (1), 270−289.
(7) Chang, W.-C.; Chen, H.-S.; Li, T.-Y.; Hsu, N.-M.; Tingare, Y. S.; Li, C.-Y.; Liu, Y.-C.; Su, C.; Li, W.-R. *Angew. Chem., Int. Ed.* **2010**, *49* (44), 8161−8164.
(8) Velazquez, H. D.; Verpoort, F. *Chem. Soc. Rev.* **2012**, *41* (21), 7032−7060.
(9) Melaiye, A.; Simons, R. S.; Milsted, A.; Pingitore, F.; Wesdemiotis, C.; Tessier, C. A.; Youngs, W. J. *J. Med. Chem.* **2004**, *47*, 973−977.
(10) Rouhi, A. M. *Chem. Eng. News* **2002**, *80* (51), 29−38.
(11) Gierz, V.; Urbanaite, A.; Seyboldt, A.; Kunz, D. *Organometallics* **2012**, *31* (21), 7532−7538.
(12) Wang, C.-Y.; Fu, C.-F.; Liu, Y.-H.; Peng, S.-M.; Liu, S.-T. *Inorg. Chem.* **2007**, *46* (14), 5779−5786.
(13) Plikhta, A.; Castillo-Molina, D. A.; Rieger, B. Ionic Liquids in Transition Metal-Catalyzed Hydroformylation Reactions. *Topics in Organometallic Chemistry*; Springer: Berlin, 2014; pp 1−50.
(14) Crudden, C. M.; Allen, D. P. *Coord. Chem. Rev.* **2004**, *248* (21−24), 2247−2273.
(15) Chang, C.-F.; Cheng, Y.-M.; Chi, Y.; Chiu, Y.-C.; Lin, C.-C.; Lee, G.-H.; Chou, P.-T.; Chen, C.-C.; Chang, C.-H.; Wu, C.-C. *Angew. Chem., Int. Ed.* **2008**, *47* (24), 4542−4545.
(16) Reindl, S. A.; Pöthig, A.; Drees, M.; Bechlars, B.; Herdtweck, E.; Herrmann, W. A.; Kühn, F. E. *Organometallics* **2013**, *32* (15), 4082−4091.
(17) Boydston, A. J.; Bielawski, C. W. *Dalton Trans.* **2006**, *34*, 4073−4077.
(18) Hofmann, P.; Brill, M. NHCP Ligands for Catalysis. *Molecular Catalysts*; Wiley-VCH Verlag GmbH & Co. KGaA: Weinheim, Germany, 2014; pp 207−234.
(19) Pugh, D.; Danopoulos, A. A. *Coord. Chem. Rev.* **2007**, *251* (5−6), 610−641.
(20) Gaillard, S.; Renaud, J.-L. *Dalton Trans.* **2013**, *42* (20), 7255−7270.
(21) Selander, N.; Szabó, K. *Chem. Rev. (Washington, DC, U. S.)* **2011**, *111* (3), 2048−2076.
(22) Morales-Morales, D.; Jensen, C. G. M. *The Chemistry of Pincer Compounds*; Elsevier Science BV: Amsterdam, The Netherlands, 2007; p 450.
(23) Chianese, A. R.; Shaner, S. E.; Tendler, J. A.; Pudalov, D. M.; Shopov, D. Y.; Kim, D.; Rogers, S. L.; Mo, A. *Organometallics* **2012**, *31* (21), 7359−7367.
(24) van der Boom, M. E. v. d.; Milstein, D. *Chem. Rev.* **2003**, *103*, 1759−1792.
(25) Gupta, M.; Hagen, C.; Flesher, R. J.; Kaska, W. C.; Jensen, C. M. *Chem. Commun. (Cambridge, U. K.)* **1996**, *17*, 2083−2084.
(26) Jensen, C. M. *Chem. Commun. (Cambridge, U. K.)* **1999**, *24*, 2443−2449.
(27) Choi, J.; MacArthur, A. H. R.; Brookhart, M.; Goldman, A. S. *Chem. Rev. (Washington, DC, U. S.)* **2011**, *111* (3), 1761−1779.
(28) Ahuja, R.; Punji, B.; Findlater, M.; Supplee, C.; Schinski, W.; Brookhart, M.; Goldman, A. S. *Nat. Chem.* **2011**, *3*, 167−171.
(29) Morales-Morales, D.; Redon, R.; Wang, Z.; Lee, D. W.; Yung, C.; Magnuson, K.; Jensen, C. M. *Can. J. Chem.* **2001**, *79*, 823−829.
(30) Haibach, M. C.; Kundu, S.; Brookhart, M.; Goldman, A. S. *Acc. Chem. Res.* **2012**, *45* (6), 947−958.
(31) Kang, P.; Cheng, C.; Chen, Z.; Schauer, C. K.; Meyer, T. J.; Brookhart, M. *J. Am. Chem. Soc.* **2012**, *134* (12), 5500−5503.
(32) Tanaka, R.; Yamashita, M.; Nozaki, K. *J. Am. Chem. Soc.* **2009**, *131*, 14168−14169.
(33) Mitton, S. J.; Turculet, L. *Chem. - Eur. J.* **2012**, *18* (48), 15258−15262.
(34) Balaraman, E.; Gunanathan, C.; Zhang, J.; Shimon, L. J. W.; Milstein, D. *Nat. Chem.* **2011**, *3*, 609−614.
(35) Ahuja, R.; Punji, B.; Findlater, M.; Supplee, C.; Schinski, W.; Brookhart, M.; Goldman, A. S. *Nat. Chem.* **2011**, *3*, 167−171.
(36) Choi, J.; Wang, D. Y.; Kundu, S.; Choliy, Y.; Emge, T. J.; Krogh-Jespersen, K.; Goldman, A. S. *Science* **2011**, *332* (6037), 1545−1548.
(37) Morales-Morales, D. *Rev. Soc. Quim. Mex.* **2004**, *48*, 338−346.
(38) Van Koten, G. *J. Organomet. Chem.* **2013**, *730*, 156−164.

DOI: 10.1021/acs.inorgchem.5b01428
Inorg. Chem. 2015, 54, 9517−9528

(39) Singleton, J. T. *Tetrahedron* **2003**, *59* (11), 1837−1857.
(40) Gunanathan, C.; Milstein, D. *Acc. Chem. Res.* **2011**, *44* (8), 588−602.
(41) Schneider, S.; Meiners, J.; Askevold, B. *Eur. J. Inorg. Chem.* **2012**, *2012* (3), 412−429.
(42) Gelman, D.; Musa, S. *ACS Catal.* **2012**, *2* (12), 2456−2466.
(43) van der Vlugt, J. I.; Reek, J. N. H. *Angew. Chem.* **2009**, *121* (47), 8990−9004.
(44) Segawa, Y.; Yamashita, M.; Nozaki, K. *J. Am. Chem. Soc.* **2009**, *131* (26), 9201−9203.
(45) Hasegawa, M.; Segawa, Y.; Yamashita, M.; Nozaki, K. *Angew. Chem., Int. Ed.* **2012**, *51* (28), 6956−6960.
(46) Masuda, Y.; Hasegawa, M.; Yamashita, M.; Nozaki, K.; Ishida, N.; Murakami, M. *J. Am. Chem. Soc.* **2013**, *135* (19), 7142−7145.
(47) Tulchinsky, Y.; Iron, M. A.; Botoshansky, M.; Gandelman, M. *Nat. Chem.* **2011**, *3* (7), 525−531.
(48) Tian, R.; Ng, Y.; Ganguly, R.; Mathey, F. *Organometallics* **2012**, *31* (6), 2486−2488.
(49) Venkanna, G. T.; Tammineni, S.; Arman, H. D.; Tonzetich, Z. J. *Organometallics* **2013**, *32* (16), 4656−4663.
(50) Dixon, L. S. H.; Hill, A. F.; Sinha, A.; Ward, J. S. *Organometallics* **2014**, *33* (3), 653−658.
(51) Whited, M. T.; Deetz, A. M.; Boerma, J. W.; DeRosha, D. E.; Janzen, D. E. *Organometallics* **2014**, *33* (19), 5070−5073.
(52) Schuster, E. M.; Botoshansky, M.; Gandelman, M. *Angew. Chem., Int. Ed.* **2008**, *47* (24), 4555−4558.
(53) Schuster, E. M.; Botoshansky, M.; Gandelman, M. *Dalton Transactions* **2011**, *40* (35), 8764−8767.
(54) Shaw, B. K.; Patrick, B. O.; Fryzuk, M. D. *Organometallics* **2012**, *31* (3), 783−786.
(55) Lee, H. M.; Zeng, J. Y.; Hu, C.-H.; Lee, M.-T. *Inorg. Chem.* **2004**, *43* (21), 6822−6829.
(56) Zeng, J. Y.; Hsieh, M.-H.; Lee, H. M. *J. Organomet. Chem.* **2005**, *690* (24−25), 5662−5671.
(57) Hahn, F. E.; Jahnke, M. C.; Pape, T. *Organometallics* **2006**, *25*, 5927−2936.
(58) Plikhta, A.; Rieger, B. Benzimidazolium-based NHC-pincer ligands. *245th ACS National Meeting & Exposition*, New Orleans, LA, 2013; American Chemical Society: Washington, DC, 2013.
(59) The green numbers indicate the size of the metallacycle, as referred to in the text.
(60) Tsvetkov, E. N.; Tkachenko, S. E.; Yarkevich, A. N. *Zurnal obscej chimii* **1988**, *58* (3), 531−536.
(61) Salem, H.; Schmitt, M.; Herrlich, U.; Kühnel, E.; Brill, M.; Nägele, P.; Bogado, A. L.; Rominger, F.; Hofmann, P. *Organometallics* **2013**, *32* (1), 29−46.
(62) Danopoulos, A. A.; Tsoureas, N.; Macgregor, S. A.; Smith, C. *Organometallics* **2007**, *26*, 253−263.
(63) Busacca, C. A.; Raju, R.; Grinberg, N.; Haddad, N.; James-Jones, P.; Lee, H.; Lorenz, J. C.; Saha, A.; Senanayake, C. H. *J. Org. Chem.* **2008**, *73*, 1524−1531.
(64) Griffin, S.; Heath, L.; Wyatt, P. *Tetrahedron Lett.* **1998**, *39*, 4405−4406.
(65) Imamoto, T.; Kikuchi, S.-i.; Miura, T.; Wada, Y. *Org. Lett.* **2001**, *3*, 87−90.
(66) El Moll, H.; Sémeril, D.; Matt, D.; Toupet, L. *Eur. J. Org. Chem.* **2010**, *2010* (6), 1158−1168.
(67) Smith, E. A. S.; Molev, G.; Botoshansky, M.; Gandelman, M. *Chem. Commun. (Cambridge, U. K.)* **2011**, *47* (1), 319−321.
(68) Labrue, F.; Pons, B.; Ricard, L.; Marinetti, A. *J. Organomet. Chem.* **2005**, *690* (9), 2285−2290.
(69) Nilsson, B. L.; Kiessling, L. L.; Raines, R. T. *Org. Lett.* **2001**, *3*, 9−12.
(70) Rahman, M. S.; Oliana, M.; Hii, K. K. *Tetrahedron: Asymmetry* **2004**, *15* (12), 1835−1840.
(71) Berthod, M.; Favre-Réguillon, A.; Mohamad, J.; Mignani, G.; Docherty, G.; Lemaire, M. *Synlett* **2007**, *2007* (10), 1545−1548.
(72) Allen, A.; Ma, L.; Lin, W. *Tetrahedron Lett.* **2002**, *43*, 3707−3710.
(73) Li, Y.; Das, S.; Zhou, S.; Junge, K.; Beller, M. *J. Am. Chem. Soc.* **2012**, *134* (23), 9727−9732.
(74) Gründemann, S.; Kovacevic, A.; Albrecht, M.; Faller, J. W.; Crabtree, R. H. *J. Am. Chem. Soc.* **2002**, *124* (35), 10473−10481.
(75) Song, G.; Li, X.; Song, Z.; Zhao, J.; Zhang, H. *Chem. - Eur. J.* **2009**, *15* (22), 5535−5544.
(76) Wolf, J.; Labande, A.; Daran, J.-C.; Poli, R. *Eur. J. Inorg. Chem.* **2008**, *2008*, 3024−3030.
(77) Arnold, P. L.; Pearson, S. *Coord. Chem. Rev.* **2007**, *251* (5−6), 596−609.
(78) Lebel, H.; Janes, M. K.; Charette, A. B.; Nolan, S. P. *J. Am. Chem. Soc.* **2004**, *126*, 5046−5047.
(79) Azua, A.; Sanz, S.; Peris, E. *Chem. - Eur. J.* **2011**, *17* (14), 3963−3967.
(80) Coumbe, T.; Lawrence, N. J.; Muhammad, F. *Tetrahedron Lett.* **1994**, *35* (4), 625−628.
(81) Chikashita, H.; Nishida, S.; Miyazaki, M.; Morita, Y.; Itoh, K. *Bull. Chem. Soc. Jpn.* **1987**, *60*, 737−746.
(82) Montgrain, F.; Ramos, S. M.; Wuest, J. D. *J. Org. Chem.* **1988**, *53*, 1489−1492.
(83) Brunet, P.; Wuest, J. D. *Can. J. Chem.* **1996**, *74*, 689−696.
(84) Mayr, M.; Buchmeiser, M. R. *Macromol. Rapid Commun.* **2004**, *25* (1), 231−236.
(85) Schwarz, D. E.; Cameron, T. M.; Hay, P. J.; Scott, B. L.; Tumas, W.; Thorn, D. L. *Chem. Commun. (Cambridge, U. K.)* **2005**, 5919−5921.
(86) Thorn, D.; Tumas, W.; Hay, J. P.; Schwarz, D.; Cameron, T. M. Method and System for hydrogen Evolution and Storage. WO 2006/009630A2, January 26, 2006.
(87) Benhamou, L.; Chardon, E.; Lavigne, G.; Bellemin-Laponnaz, S. p.; César, V. *Chem. Rev. (Washington, DC, U. S.)* **2011**, *111* (4), 2705−2733.
(88) Bildstein, B.; Malaun, M.; Kopacka, H.; Ongania, K.-H.; Wurst, K. *J. Organomet. Chem.* **1999**, *572*, 177−187.
(89) Frech, C. M.; Shimon, L. J. W.; Milstein, D. *Helv. Chim. Acta* **2006**, *89* (8), 1730−1739.
(90) Swatloski, R. P.; Holbrey, J. D.; Rogers, R. D. *Green Chem.* **2003**, *5* (4), 361−363.
(91) Huddleston, J. G.; Visser, A. E.; Reichert, W. M.; Willauer, H. D.; Broker, G. A.; Rogers, R. D. *Green Chem.* **2001**, *3* (4), 156−164.
(92) Adams, J. J.; Arulsamy, N.; Roddick, D. M. *Organometallics* **2009**, *28* (4), 1148−1157.
(93) Albinati, A.; Chaloupka, S.; Eckert, J.; Venanzi, L. M.; Wolfer, M. K. *Inorg. Chim. Acta* **1997**, *259*, 305−316.
(94) Ho, H.-A.; Manna, K.; Sadow, A. D. *Angew. Chem.* **2012**, *124*, 8735−8738.
(95) Polukeev, A. V.; Petrovskii, P. V.; Peregudov, A. S.; Ezernitskaya, M. G.; Koridze, A. A. *Organometallics* **2013**, *32* (4), 1000−1015.
(96) Morales-Morales, D.; Redón, R.; Wang, Z.; Lee, D. W.; Yung, C.; Magnuson, K.; Jensen, C. M. *Can. J. Chem.* **2001**, *79* (5−6), 823−829.
(97) Kloek, S. M.; Heinekey, D. M.; Goldberg, K. I. *Organometallics* **2006**, *25*, 3007−3011.
(98) Adams, J. J.; Arulsamy, N.; Roddick, D. M. *Organometallics* **2012**, *31* (4), 1439−1447.
(99) Çelenligil-Çetin, R.; Watson, L. A.; Guo, C.; Foxman, B. M.; Ozerov, O. V. *Organometallics* **2005**, *24* (2), 186−189.
(100) Huang, K.-W.; Grills, D. C.; Han, J. H.; Szalda, D. J.; Fujita, E. *Inorg. Chim. Acta* **2008**, *361* (11), 3327−3331.
(101) Cid, J.; Carbó, J. J.; Fernández, E. *Chem. - Eur. J.* **2012**, *18* (5), 1512−1521.
(102) Gunanathan, C.; Hölscher, M.; Pan, F.; Leitner, W. *J. Am. Chem. Soc.* **2012**, *134* (35), 14349−14352.
(103) Takaya, J.; Kirai, N.; Iwasawa, N. *J. Am. Chem. Soc.* **2011**, *133* (33), 12980−12983.
(104) Lee, C.-I.; Zhou, J.; Ozerov, O. V. *J. Am. Chem. Soc.* **2013**, *135* (9), 3560−3566.
(105) Zhang, L.; Zuo, Z.; Wan, X.; Huang, Z. *J. Am. Chem. Soc.* **2014**, *136* (44), 15501−15504.

DOI: 10.1021/acs.inorgchem.5b01428
Inorg. Chem. 2015, 54, 9517−9528

(106) Obligacion, J. V.; Chirik, P. J. *J. Am. Chem. Soc.* **2013**, *135* (51), 19107−19110.
(107) Bruneau, C.; Dixneuf, P. H. *Angew. Chem., Int. Ed.* **2006**, *45* (14), 2176−2203.
(108) Sun, C.; Liu, M.; Sun, H.; Hang, F.; Sun, N.; Chen, D. *Int. J. Quantum Chem.* **2015**, *115* (2), 59−67.
(109) *APEX 2: APEX suite of crystallographic software*, version 2008.4; Bruker AXS Inc.: Madison, WI, 2008.
(110) *SAINT*, version 7.56a; Bruker AXS Inc.: Madison, WI, 2008. *SADABS*, version 2008/1; Bruker AXS Inc.: Madison, WI, 2008.
(111) Sheldrick, G. M. *SHELXS-97, Program for Crystal Structure Solution*; University of Göttingen: Göttingen, Germany, 1997.
(112) Sheldrick, G. M. *SHELXL-97*; University of Göttingen: Göttingen, Germany, 1997.
(113) Huebschle, C. B.; Sheldrick, G. M.; Dittrich, B. *J. Appl. Crystallogr.* **2011**, *44*, 1281−1284.
(114) *International Tables for Crystallography*; Wilson, A. J. C., Ed.; Kluwer Academic Publishers: Dordrecht, The Netherlands, 1992; Vol. *C*, Tables 6.1.1.4 (pp 500−502), 4.2.6.8 (pp 219−222), and 4.2.4.2 (pp 193−199),
(115) Spek, A. L. *PLATON, A Multipurpose Crystallographic Tool*; Utrecht University: Utrecht, The Netherlands, 2010.

DOI: 10.1021/acs.inorgchem.5b01428
Inorg. Chem. 2015, 54, 9517−9528